ACS OMEGA

Open Access

http://pubs.acs.org/journal/acsodf

Article

Improved Targeting and Safety of Doxorubicin through a Novel Albumin Binding Prodrug Approach

Yang Liu,[⊥] Sergio Corrales-Guerrero,[⊥] Jimmy C. Kuo, Ryan Robb, Gregory Nagy, Tiantian Cui, Robert J. Lee,* and Terence M. Williams*

Cite This: *ACS Omega* 2024, 9, 977−987

Read Online

ACCESS | Metrics & More | Article Recommendations | Supporting Information

ABSTRACT: Human serum albumin (HSA) improves the pharmacokinetic profile of drugs attached to it, making it an attractive carrier with proven clinical success. In our previous studies, we have shown that Caveolin-1 (Cav-1) and caveolae-mediated endocytosis play important roles in the uptake of HSA and albumin-bound drugs. Doxorubicin is an FDA-approved chemotherapeutic agent that is effective against multiple cancers, but its clinical applicability has been hampered by its high toxicity levels. In this study, a doxorubicin-prodrug was developed that could independently and avidly bind HSA in circulation, called IPBA-Dox. We first developed and characterized IPBA-Dox and confirmed that it can bind albumin in vitro while retaining a potent cytotoxic effect. We then verified that it efficiently binds to HSA in circulation, leading to an improvement in the pharmacokinetic profile of the drug. In addition, we tested our prodrug for Cav-1 selectivity and found that it preferentially affects cells that express relatively higher levels of Cav-1 in vitro and in vivo. Moreover, we found that our compound was well tolerated in vivo at concentrations at which doxorubicin was lethal. Altogether, we have developed a doxorubicin-prodrug that can successfully bind HSA, retaining a strong cytotoxic effect that preferentially targets Cav-1 positive cells while improving the general tolerability of the drug.

1. INTRODUCTION

Human serum albumin (HSA) is the most abundant protein in plasma, with a relatively long half-life of 19 days in the circulation. HSA has been shown to improve the pharmacokinetic profile of drugs bound to it[1−3] and it has been well established that HSA naturally accumulates in tumors due to abnormal angiogenesis and leaky vasculature of solid tumors, which is known as the enhanced permeability and retention effect (EPR).[4−6] In addition to this form of tumor targeting, cancer cells can readily take up HSA via caveolae-mediated endocytosis.[7−12] Because of these properties, HSA is an interesting drug carrier candidate for the development of novel chemotherapeutic approaches to cancer treatment.

Caveolin-1 (Cav-1) is the main structural component of caveolae and is crucial for caveolae-mediated endocytosis. Caveolae are small (50−100 nm) flask-shaped invaginations in the plasma membrane that are important for cholesterol homeostasis, nutrient uptake, and signal transduction.[7,13−15] Importantly, Cav-1 has been found to be upregulated in several cancer types including pancreatic adenocarcinomas, breast cancer, and nonsmall cell lung cancers, among others.[16−22] In addition, Cav-1 has been found to be associated with worse clinical outcomes in certain cancer types.[17−20,22−27] Finally, previous work from our group showed that Cav-1 expression is crucial for the uptake of HSA and HSA-bound chemotherapies, thereby potentially serving as a biomarker for response to these treatments.[7,12,28] Recently, we and others demonstrated that Cav-1 may serve as a biomarker for response to albumin-bound or conjugated chemotherapy in multiple clinical cohorts.[29−31]

Doxorubicin is a potent antitumor agent that is effective against a broad range of cancers.[32] However, clinical use of doxorubicin has been hampered by dose-limiting adverse effects such as, but not limited to, myelosuppression and cardiotoxicity.[33,34] Additionally, the pharmacokinetic characteristics of doxorubicin include a short half-life in circulation, which limits its potential effects.[35] In recent years, several mechanisms have been developed to overcome these disadvantages, particularly focusing on delivery mechanisms, including liposomes, polymeric nanoparticles, antibody-conjugated drugs, and prodrugs.[36−45] Here, we rationally developed a doxorubicin-prodrug (IPBA-Dox) that can bind albumin in the serum both in vitro and in vivo. This novel molecule, characterized by a 4-(*p*-iodophenyl) butyric acid linker, showed an improved pharmacokinetic profile over its parental drug, while remaining a powerful antitumor agent. Moreover, our studies suggest that IPBA-Dox preferentially targets cancer cells that express high levels of Cav-1, confirming the therapeutic advantage of HSA as a drug carrier and providing additional evidence that Cav-1 may serve as a potential biomarker for this type of therapy.

Received: September 18, 2023
Revised: December 8, 2023
Accepted: December 12, 2023
Published: December 21, 2023

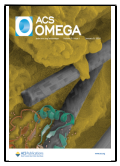

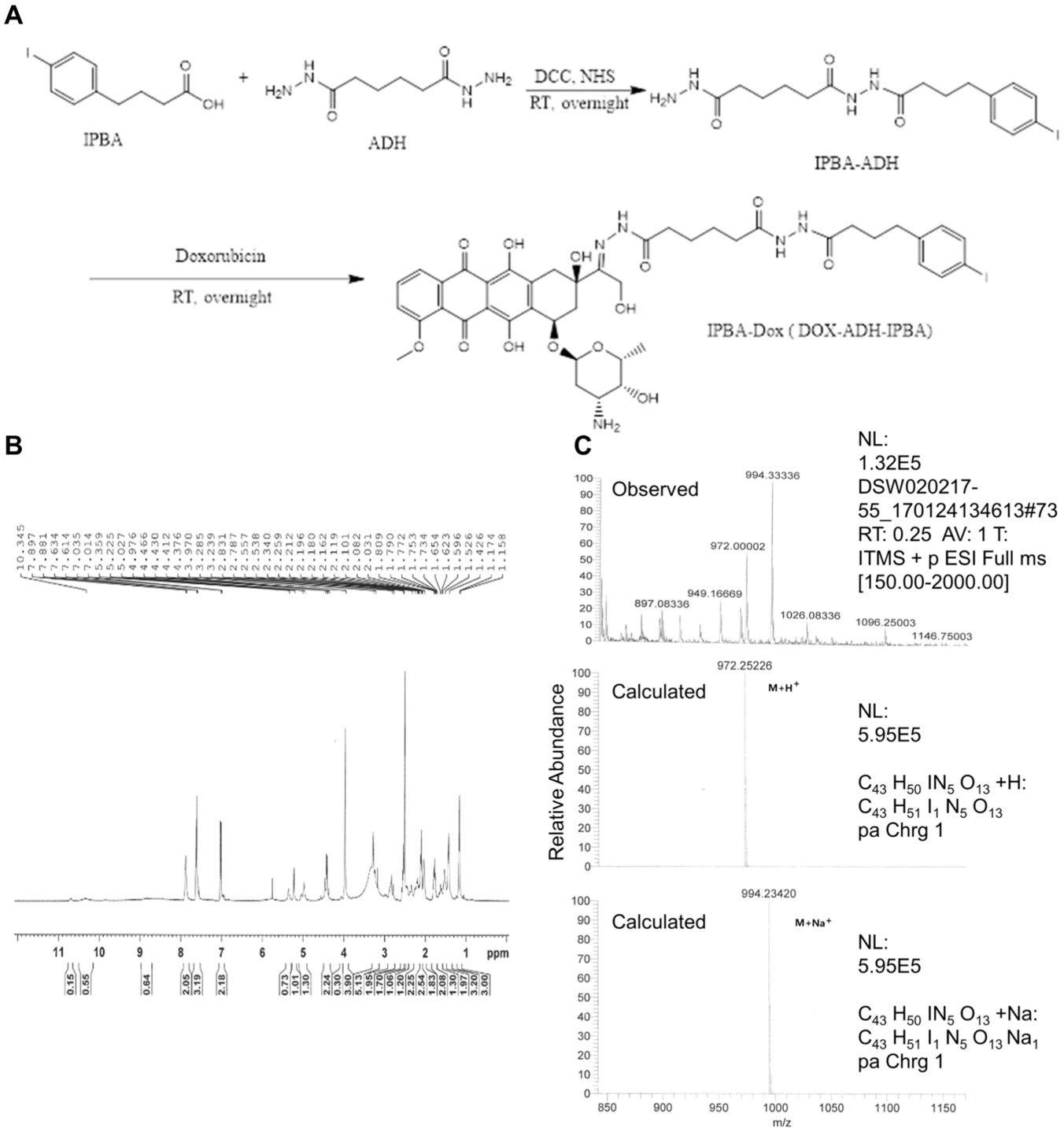

Figure 1. Characterization of IPBA-Dox: (A) synthesis steps of IPBA-Dox. The first step consists of generation of the acid-sensitive linker, which is then bound to doxorubicin in the second step. (B) ^{1}H NMR spectrum: proton nuclear magnetic resonance characterization of the new molecule: ^{1}H NMR 7.89 (m, 2H), 7.62 (d, 3H), 7.02 (d, 2H), 5.36 (s, 1H), 5.22 (s, 1H), 5.00 (d, 1H), 4.42 (m, 2H), 3.97 (s, 4H), 3.28−3.24 (m, 7H), 2.81 (m, 2H), 2.56 (m, 1H), 2.34−2.03 (m, 8H), 1.81−1.43 (m, 8H), 1.16 (d, 3H). (C) ESI-MS mass spectrum using an electrospray ionization source.

2. RESULTS

2.1. Characterization of IPBA-Dox. The reaction scheme for the synthesis of IPBA-Dox is shown in Figure 1A and described in the Methods section. Following synthesis, we characterized our newly developed molecule with a 300 MHz ^{1}H Nuclear Magnetic Resonance (NMR) spectroscope (Figure 1B). The mass spectrum was acquired using an electrospray ionization source (ESIMS): m/z = 972.2 [M + H$^+$] and 994.3 [M + Na$^+$] and matched the proposed structure (Figure 1C). As expected, this is higher than the molecular weight of doxorubicin (397).[46] Finally, the stability of IPBA-Dox was studied with high- and low-quality-control (QC) samples under freeze−thaw, short-term (24 h) room temperature, and long-term (4 week) low temperature conditions (Table 1). The variability found in the results for these conditions is well within the acceptable degree of assay variability (the acceptable limit for accuracy is set as 85−115%).

https://doi.org/10.1021/acsomega.3c07163
ACS Omega 2024, 9, 977−987

Table 1. Freeze-Thaw Cycle, Room Temperature, and Low Temperature Stability

		freeze-thaw cycle		24 h room temperature		4-week at −20°C	
		LQC (10 ng/mL)	HQC (1000 ng/mL)	LQC (10 ng/mL)	HQC (1000 ng/mL)	LQC (10 ng/mL)	HQC (1000 ng/mL)
DOX	mean	9.12	975.8	9.82	997	9.615	1026.8
	% CV	5.7	4.81	5.14	2.24	4.22	3.3
	% accuracy	91.2	97.58	98.23	99.7	96.15	102.68
IPBA-Dox	mean	9.01	901.5	9.64	1012	9.77	945.5
	% CV	3.17	3.75	4.8	5.17	5.81	7.93
	% accuracy	90.1	90.15	96.35	101.2	97.65	94.55

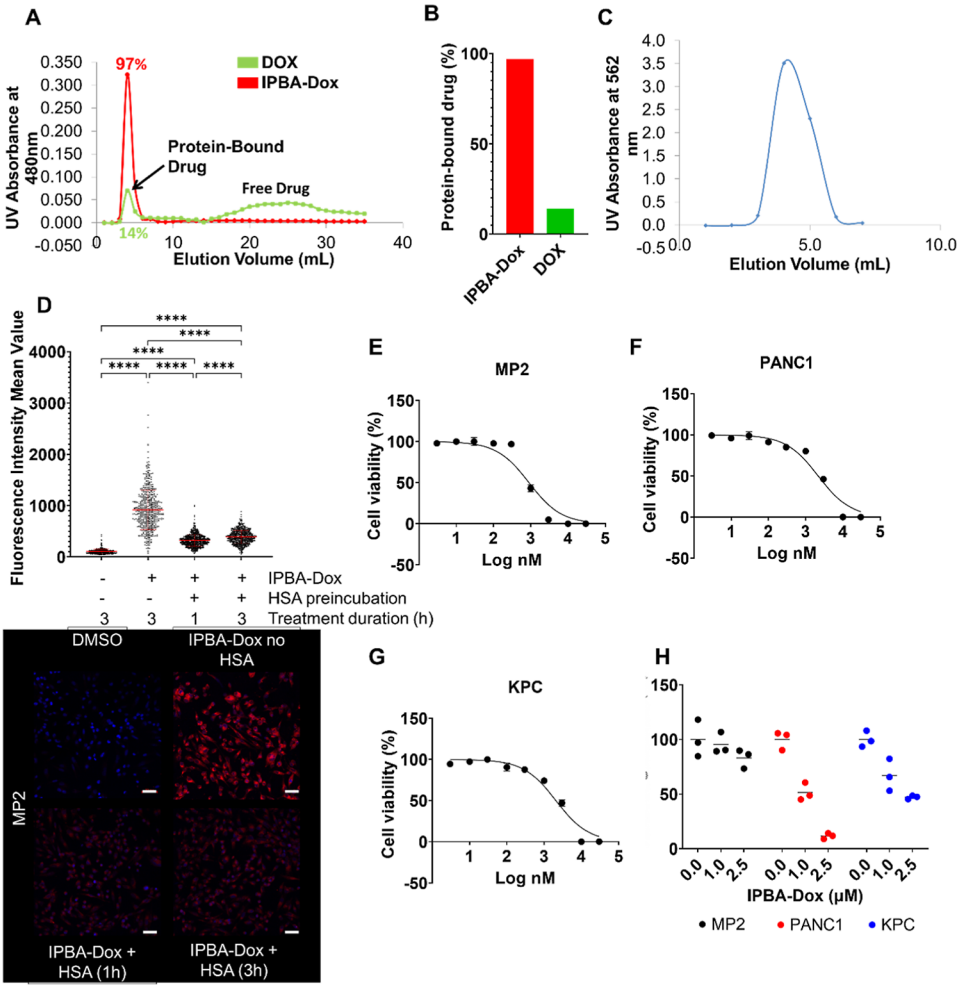

Figure 2. IPBA-Dox binds in vitro to albumin and retains cytotoxicity: (A) HSA-binding efficiency calculated for doxorubicin and IPBA-Dox using gel filtration chromatography and measuring each fraction at UV−vis 480 nm. (B) Representative histogram of percentage of eluted drug that was bound to protein fraction (HSA). (C) BCA protein assay on early chromatography fractions as measured by UV absorbance at 562 nm. (D) Quantification of red fluorescent signal observed in MP2 cells after treatment with IPBA-Dox with or without preincubation with HSA prior to cell treatment (final HSA concentration of 0.5% in well), $n > 450$ cells, ****: $p < 0.0001$. Representative microscopy images shown below. Scale bar, 50 μm. (E−G) Cell viability assays of MP2, PANC1, and KPC cells treated with IPBA-Dox in complete medium for 72 h. (H) Colony formation assay of MP2, PANC1, and KPC cells treated with IPBA-Dox for 48 h in complete medium, normalized to mean colonies under control (vehicle) conditions.

The stability of doxorubicin and prodrug in plasma samples was investigated with high (H) and low (L) QC samples under three conditions: freeze−thaw, short-term room temperature (RT), and long-term low temperature ($n = 4$ per group). CV = coefficient of variation.

2.2. IPBA-Dox Binds Albumin Avidly while Retaining Cytotoxic Efficacy In Vitro. To determine the IPBA-Dox binding efficiency, we compared the HSA binding of IPBA-Dox to that of doxorubicin. First, we incubated the drugs with HSA at 37 °C for 60 min and then analyzed them by gel filtration chromatography, measuring each fraction at UV−vis 480 nm. We observed an albumin-binding efficiency of 97% for our IPBA-Dox, in contrast to 14% for doxorubicin (Figure 2A,B). To confirm that the peaks of the drug observed correspond to the protein-bound drug, we performed BCA assays on the first 7 fractions (1.0 mL per fraction) to determine protein concentrations and found that fractions 3−6 correspond to protein molecules (Figure 2C). To further

https://doi.org/10.1021/acsomega.3c07163
ACS Omega 2024, 9, 977−987

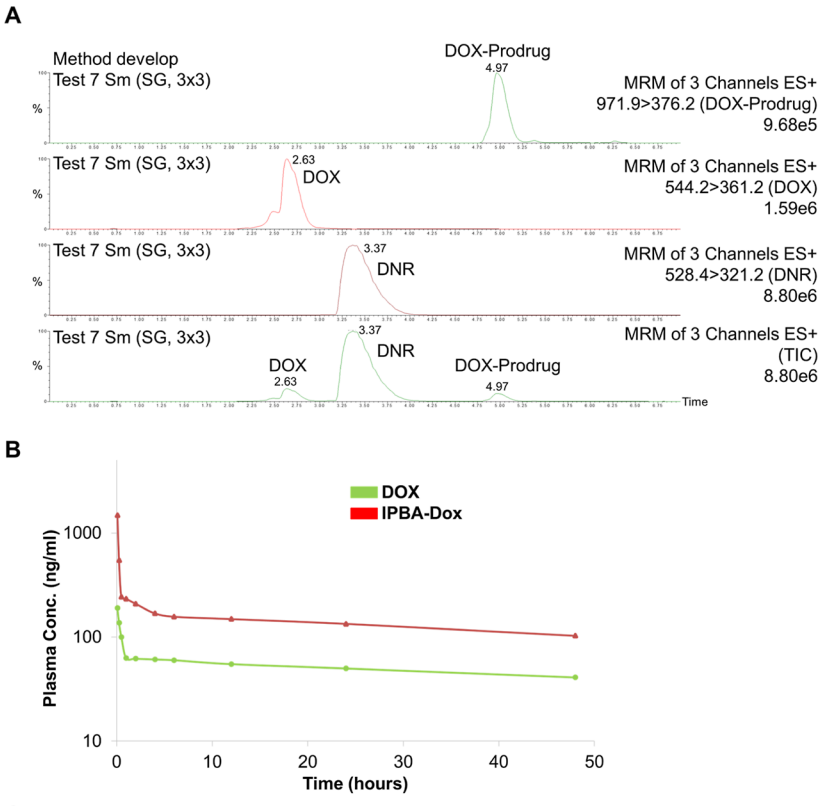

C

PK Parameters	Free doxorubicin	IPBA-Dox
C_{max}(μg/mL)	0.27 ± 0.09	2.55 ± 0.32
AUC(hr*μg/mL)	0.26 ± 0.02	2.90 ± 0.65
$T_{1/2\alpha}$(min)	2.7 ± 0.9	5.4 ± 0.7
$T_{1/2\beta}$(hr)	3.21 ± 0.41	17.5 ± 5.4
CL(L/hr/kg)	23.4 ± 2.1	3.44 ± 0.78
V_{ss}(L/kg)	102.6 ± 6.5	77.6 ± 12.4

Figure 3. Pharmacokinetic study of IPBA-Dox: (A) representative chromatogram of the LC−MS/MS analysis method developed on IPBA-Dox (DOX-Prodrug) and doxorubicin (DOX) in mice plasma, with daunorubicin (DNR) as control. (B) Pharmacokinetic profiles of doxorubicin and IPBA-Dox in mouse plasma over time. Curves represent the plasma concentration of the drug over time. (C) Comparative pharmacokinetic parameters analyzed using a two-compartment model.

validate that IPBA-Dox can bind HSA, we compared the uptake dynamics of IPBA-Dox with or without HSA preincubation in MIAPaCa-2 (MP2) cells using confocal microscopy to evaluate the autofluorescent signal intrinsic to doxorubicin. We found that in cells cultured in serum-free media to prevent competition from bovine serum albumin (BSA), cells treated with IPBA-Dox that were not preincubated with HSA had the highest levels of doxorubicin uptake at up to 3 h, suggesting free drug transit of IPBA-Dox across membranes (Figure 2D). As expected, cells treated with IPBA-Dox that were preincubated with HSA (final HSA concentration in well = 0.5%) had a reduced uptake signal, suggesting that the uptake mechanism had changed from passive transit of free drug to a protein-mediated uptake mechanism (Figure 2D). Notably, we observed a time-dependent increase in the doxorubicin autofluorescence signal from 1 to 3 h.

Next, in order to verify that our modification of doxorubicin still possessed significant cytotoxic properties to tumor cells, we not only examined the cell viability of human pancreatic cancer cell lines MIA-PaCa2 (MP2) and PANC1, but also murine $KRAS^{G12D}$ $Trp53^{R270H}$ PDX1-Cre (KPC) cells, isolated from mouse pancreatic tumors in our laboratory, after treatment with IPBA-Dox. We observed that the compound was highly efficient in promoting cytotoxicity, resulting in IC50 values of 898.1, 2178, and 2076 nM, respectively (Figure 2E−G). Lastly, in order to confirm the cytotoxic effects, we performed colony formation assays by treating MP2, PANC1, and KPC cells with increasing doses of IPBA-Dox for 48 h. We observed that IPBA-Dox was cytotoxic in dose- and cell-line-dependent manners (Figure 2H). Taken together, our results indicate that our novel IPBA-Dox avidly binds HSA with substantially higher affinity than the parental drug while retaining a highly efficient cytotoxic profile.

2.3. IPBA-Dox Shows Enhanced In Vivo Pharmacokinetics. To establish the pharmacokinetic profile of IPBA-Dox, a highly sensitive and robust LC−MS/MS assay was established for the simultaneous measurement of doxorubicin and IPBA-Dox concentrations in mouse plasma over a period of 48 h (Figures 3A and S1−S3, Supporting Information). The plasma concentrations of doxorubicin and IPBA-Dox (dosed at equivalent molar doses) were assessed over time (Figure 3B), in which a steep distribution phase was initially observed followed by a long terminal elimination phase. The comparative pharmacokinetic parameters analyzed by using the two-compartment model are presented in Figure 3C.

https://doi.org/10.1021/acsomega.3c07163
ACS Omega 2024, 9, 977−987

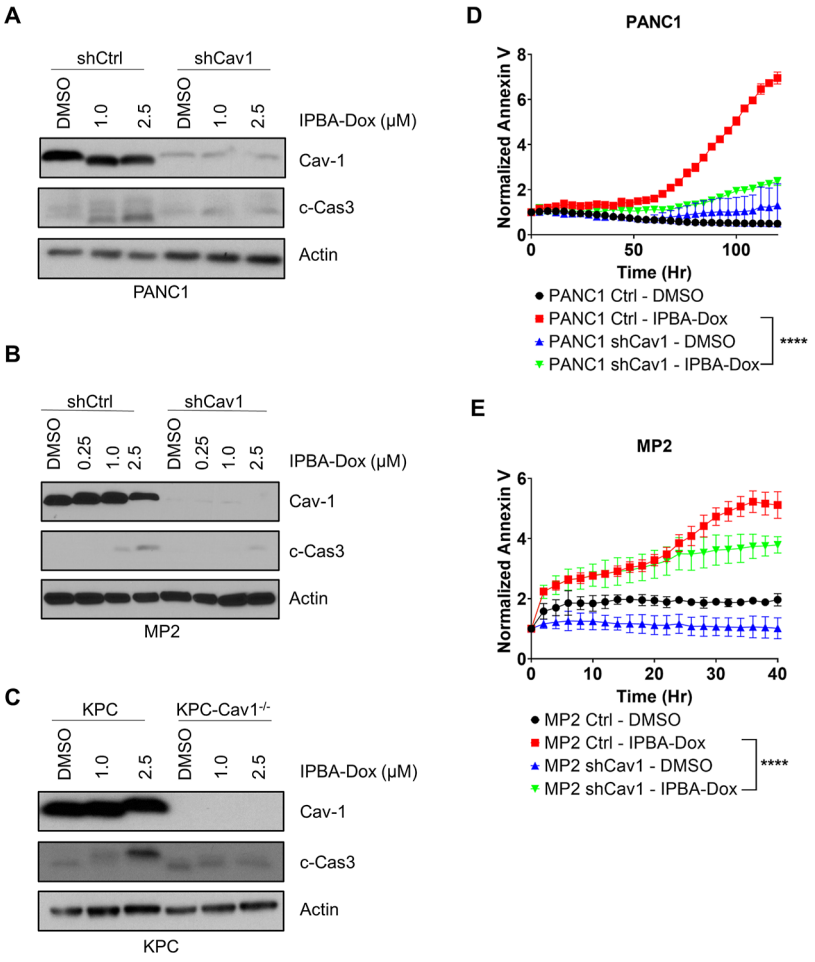

Figure 4. IPBA-Dox demonstrates increased cytotoxicity against cells with higher Cav-1 expression: (A−C) Western blotting showing levels of cleaved caspase-3 (c-Cas3) of MP2, PANC1, and KPC isogenic cell line pairs after 72 h of treatment with IPBA-Dox in complete medium. (D,E) Quantification of fluorescent Annexin V signal by live-cell imaging of PANC1 or MP2 cells treated with 0.1 or 2.5 μM of IPBA-Dox, respectively. One of multiple independent experiments is shown per cell line. ****: $p < 0.0001$.

IPBA-Dox produced an approximately 10-fold higher AUC, $T_{1/2\alpha}$ of 5.4 min and $T_{1/2\beta}$ of 17.5 h, while free drug (parental) generated $T_{1/2\alpha}$ of 2.7 min and $T_{1/2\beta}$ of 3.21 h. The terminal plasma half-life of the prodrug was 5.5-fold more than that of the free drug. The steady-state volume of distribution (V_{ss}) with the prodrug was 77.6 L/kg compared to 102.6 L/kg with the free drug or about 1.5-fold less than that of free doxorubicin, while the clearance rate was substantially lower with the prodrug. This data suggest that the IPBA-Dox can bind albumin with high affinity in vivo, thereby improving its pharmacokinetic profile.

2.4. IPBA-Dox Shows In Vitro Selectivity for High Cav-1-Expressing Tumor Cells. In our previous work, we established the importance of Cav-1 and caveolae-mediated endocytosis for HSA uptake and consequently HSA-bound drugs.[7,12] In these studies, we have shown that drugs bound or conjugated to HSA have a higher uptake and subsequent cytotoxic effect on cells expressing relatively higher Cav-1 levels, nominating Cav-1 as a potential biomarker of this class of therapeutics. To confirm whether these previous observations would extend to molecules that would independently bind to albumin, we studied the cytotoxic effect of IPBA-Dox in PANC1 and MP2 cells with genetically depleted Cav-1 levels by shRNA. We also complemented these studies in pancreatic cancer cells isolated from pancreatic tumors arising in $KRAS^{G12D}$ $Trp53^{R270H}$ PDX1-Cre genetically engineered mice, either with Cav-1 ("KPC") or without Cav-1 ("KPC-$Cav1^{-/-}$"). Human and mouse pancreatic cancer cell lines were treated with increasing doses of IPBA-Dox for 72 h, and cleaved caspase-3 levels were assessed by Western blotting as a marker of apoptosis induction. As expected, we observed that cells that had relatively higher levels of Cav-1 demonstrated higher levels of cleaved caspase-3 (Figure 4A−C).

To further investigate our findings, we performed live-cell imaging using a fluorescent reporter for Annexin V (an early marker of apoptosis). We similarly observed that cells expressing higher Cav-1 had a higher fluorescent signal, confirming higher levels of apoptosis in the Cav-1-proficient cells compared to the Cav-1-depleted cells (Figure 4D,E). Taken together, these results suggest that cells expressing relatively higher levels of Cav-1 are more sensitive to IPBA-Dox in vitro, in agreement with previous studies we performed on other albumin-bound chemotherapies.

2.5. IPBA-Dox is Effective In Vivo and Preferentially Reduces Tumor Growth in High Cav-1 Expressing Tumors. To explore the efficacy of our novel IPBA-Dox as an antitumor agent in vivo, we heterotopically injected KPC and KPC-$Cav1^{-/-}$ isogenic pancreatic cancer cell lines into athymic nude mice. After tumor formation, the mice were randomized and treated with vehicle, doxorubicin (parental

https://doi.org/10.1021/acsomega.3c07163
ACS Omega 2024, 9, 977−987

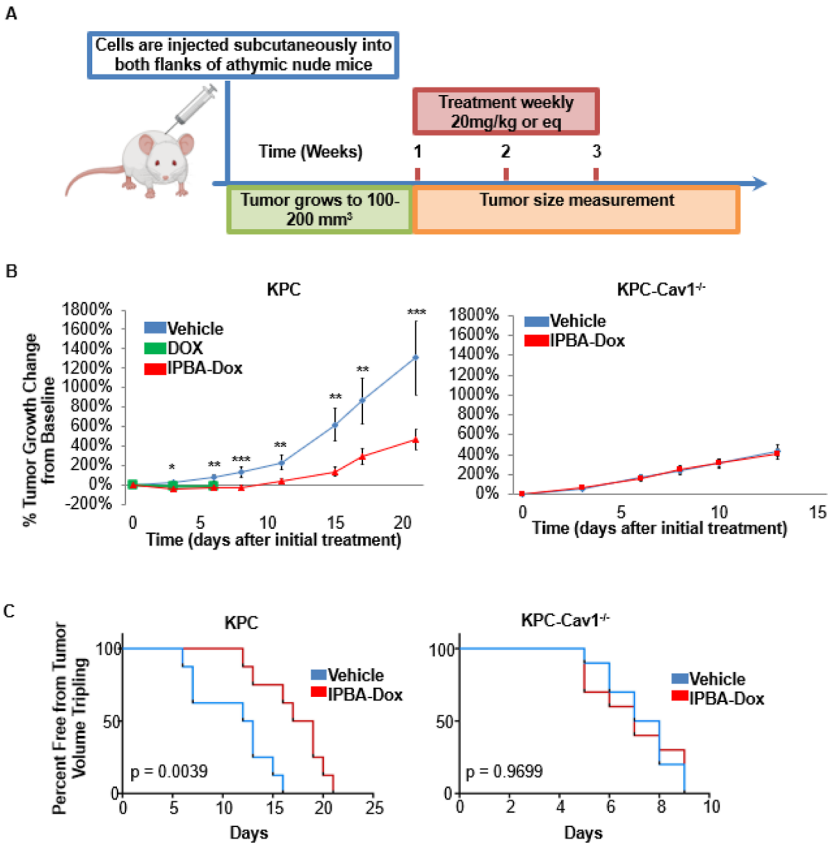

Figure 5. IPBA-Dox demonstrates increased tolerability compared to doxorubicin and enhanced effect in Cav-1 tumors in an (A) in vivo treatment scheme. Mice were treated weekly for 3 weeks with vehicle, 20 mg/kg doxorubicin, or IPBA-Dox (20 mg/kg doxorubicin equivalent, "eq") via IV injections. (B) Average sizes of KPC and KPC-Cav-1$^{-/-}$ tumors over time from initial treatment (n = 8−10 tumors per group) normalized to baseline pretreatment size. *: $p < 0.05$, **: $p < 0.01$, ***: $p < 0.001$. (C) Kaplan−Meier survival curves show percentage of mice free from tumor volume tripling.

drug), or IPBA-Dox at equivalent molar doses of 20 mg/kg doxorubicin (Figure 5A). IPBA-Dox was tolerable and significantly reduced the tumor growth rate of KPC tumors, while doxorubicin induced toxicity-related fatality in all mice at that dose within 1 week (Figure 5B, left panel). Moreover, IPBA-Dox significantly increased the time to tumor volume tripling in KPC tumors (Figure 5C, left panel). In KPC-Cav1$^{-/-}$ tumors, no differences in the growth rate or time to tumor tripling were observed (Figure 5B,C, right panels). In both groups of mice, IPBA-Dox was well tolerated, with minimal weight changes and signs of clinical toxicity found at the 20 mg/kg equimolar dosing (Figure S4A,B). Taken together, these experiments confirm that IPBA-Dox is a significantly more tolerable compound than doxorubicin at equimolar doses, that IPBA-Dox is an efficacious antitumor agent, and that Cav-1 expression may serve as a biomarker to predict the enhanced response of tumors to IPBA-Dox.

3. DISCUSSION

Doxorubicin is a highly effective antitumor agent with activity against a broad spectrum of human cancers. However, its clinical use is affected by dose-limiting adverse effects, including cumulative cardiotoxicity and myelosuppression. Pharmacokinetic studies have indicated doxorubicin has a very short half-life in the blood and is taken up by cardiac muscles.[35,47] It is well established that albumin, the most abundant protein in plasma, is a natural transporter of nutrients with a very high circulatory half-life of 19 days. Albumin-bound drugs are thought to be preferentially delivered to solid tumor cells due to the EPR effect and the amplified expression of albumin-binding proteins on the tumor endothelium and tumor cells.[11,48,49] In addition, tumor cells frequently overexpress Cav-1, which enhances the internalization of albumin-associated drugs through caveolae-mediated endocytosis.[7,12] The latter mechanism and other uptake mechanisms are likely to increase in a harsh, competitive tumor microenvironment as tumor cells scavenge nutrients. Herein, IPBA-Dox, a novel albumin-binding prodrug, was designed to improve the therapeutic index of doxorubicin. This prodrug has two distinct features: high-efficiency binding of circulating endogenous serum albumin (extending its plasma half-life) and release of doxorubicin at the tumor by virtue of the acid-sensitive linker between the drug and the binding tag and tumor-cell-related endocytosis of albumin. Taken together, these features lead to reduced toxicity and improved therapeutic efficacy in vivo.

The pharmacokinetics of doxorubicin has been reported to be very complex (three-compartment model behavior) and characterized by rapid drug clearance from plasma after intravenous injection.[35,47,50] To further understand the strengths of IPBA-Dox compared to the free drug, a preclinical pharmacokinetic study on mice was conducted (Figure 3), and a sensitive and validated LC−MS/MS assay was established for measuring doxorubicin and IPBA-Dox plasma concentrations (Figures S1−S3 and Supporting Information). This analytical method offers marked advantages over previously reported

https://doi.org/10.1021/acsomega.3c07163
ACS Omega 2024, 9, 977−987

approaches, namely, spectrophotometric measurement[51,52] and HPLC-FL,[53] by dramatically increasing the drug detection sensitivity for extremely low plasma drug concentrations at the ng/mL level and substantially improving assay specificity (by eliminating interference from the matrix, drug degradants, and in vivo metabolites). In our pharmacokinetic study, the area under the plasma concentration (AUC) versus time curve for IPBA-Dox and doxorubicin (at doxorubicin equivalent doses) were 2.90 and 0.26 h μg/mL, respectively, representing an approximately 7-fold increase. This was further reflected in the long terminal half-life of IPBA-Dox (17.5 h) compared to that of doxorubicin (3.2 h). In addition, IPBA-Dox had a much lower clearance rate of 3.44 L/h/kg, reflecting an ∼7-fold reduction compared to free doxorubicin. These pharmacokinetic results suggest that IPBA-Dox can bind to circulating albumin with high affinity in vivo and prolong its systemic circulation time, thus potentially improving the chemotherapeutic efficacy of the drug while decreasing its toxicity to off-target organs.

Indeed, we found that IPBA-Dox could be used at equivalent doses higher than that of the parental doxorubicin drug in our in vivo experiments (Figure 5). Additionally, treatment with IPBA-Dox led to a significant reduction in tumor growth, while prolonging the time required for tumor volume tripling (a surrogate of survival in our study). This was observed in models expressing endogenous Cav-1, which was lost when Cav-1 was genetically depleted. This Cav-1-dependent effect, which was also observed in vitro (Figure 4), agrees with previous results from our group, where we have shown the importance of Cav-1 in the uptake of albumin and albumin-related drugs.[7,12,28] Also, this reinforces the concept that Cav-1 may serve as a potential predictive biomarker for albumin-bound or albumin-conjugated chemotherapies. Importantly, Cav-1 has been found to be upregulated in various cancer types, such as sarcomas, pancreatic, lung, and other cancers,[16−22] and has been associated with worse outcomes.[17−20,22−27] Future studies should be focused on developing a better understanding of the subcellular trafficking process of this albumin-Dox conjugate through the plasma membrane, caveosomes, lysosomes, and so forth, and at which point doxorubicin is released to transit to the nucleus.

Recently, other doxorubicin prodrugs have also been developed. These drugs were designed with a maleimide group to react with the thiol group of cysteine 34 on albumin, generating a covalent bond between albumin and the prodrug.[44,54,55] The most notable of these compounds is the (6-maleimidocaproyl) hydrozone derivative aldoxorubicin, which is currently in phase III clinical trials. In this case, doxorubicin has been conjugated to 6-maleimidocaproic acid hydrazide, which also serves as an acid-sensitive linker. However, it is generally known that several other sulfhydryl compounds may react with aldoxorubicin via the same reaction mechanism, potentially hampering the full potential of this prodrug. Therefore, noncovalent binding strategies for albumin have been developed.[56,57] Of particular interest is the class of 4-(*p*-iodophenyl) butyric acid (IPBA) analogs that have shown stable noncovalent albumin-binding properties with both human and mouse albumin.[58] Therefore, we rationally designed our novel IPBA-Dox using an IPBA analogue to serve as an albumin binder. The difference in the albumin-binding mechanism between aldoxorubicin and IPBA-Dox is sufficient to establish that IPBA-Dox is a novel compound.

In conclusion, we designed a novel doxorubicin-prodrug with the following goals: (1) to avidly bind endogenous albumin, (2) to enhance delivery in tumors through EPR and upregulated tumor endocytic mechanisms (i.e., caveolae-mediated endocytosis), and (3) to release the doxorubicin payload into the acidic tumor microenvironment. Our results show that IPBA-Dox has a favorable pharmacokinetic profile over doxorubicin, safer dosing capabilities, and importantly, significant antitumor effects in our preclinical models. Taken together, these results suggest that IPBA-Dox is an interesting candidate for further preclinical and clinical studies.

4. MATERIALS AND METHODS

4.1. Materials and Reagents. Doxorubicin and fetal bovine serum (FBS) were purchased from Sigma-Aldrich (St. Louis, MO). Daunorubicin was purchased from Cayman Chemical Co. (Ann Arbor, MI). BD syringes and needles, HPLC grade water, methanol, acetonitrile, LC−MS grade formic acid, methanol, DMSO, DMF, and other organic solvents were obtained from Fisher Scientific (Hampton, NH). 4-(*p*-Iodophenyl) butyric acid (IPBA) was purchased from Santa Cruz (Dallas, TX). Adipic acid dihydrazide (ADH) was purchased from Sigma-Aldrich (St. Louis, MO). Heparin was obtained from Pfizer (New York, NY). Dulbecco's Modified Eagle Medium (DMEM) and phosphate-buffered saline (PBS) were purchased from GE healthcare Bio-Sciences (Pittsburgh, PA). 0.25% w/v trypsin/1 mM EDTA was purchased from Gibco Life Technologies (Grand Island, NY).

4.2. IPBA-Dox Synthesis. Ten mg 4-(*p*-iodophenyl) butyric acid (IPBA) was dissolved in 1 mL chloroform in a 5 mL round-bottom flask. 8.5 mg DCC and 4.8 mg NHS were added to the solution, and the mixture was stirred at room temperature overnight. The DCU precipitate was removed, and 6 mg of ADH in DMF was added to the mixture. Ten mg of doxorubicin was added after 4 h, and the mixture was stirred overnight at room temperature. The reaction was monitored by aluminum oxide TLC with a mobile phase mixture of chloroform/methanol/glacial acetic acid (80:20:5 ratio). The product was purified by column chromatography on a silica gel column with methanol and chloroform (1:4 v/v) in a yield of 51%. Product was analyzed in solvent $CDCl_3$ by Nuclear Magnetic Resonance spectroscope, Bruker 300 MHz (Billerica, MA), and characterized in 0.1% formic acid/acetonitrile mixture by Waters Quattro Premier Mass Spectrometer (Milford, MA) in positive ion mode (capillary voltage 3.0 kV and cone voltage 30 V).

4.3. IPBA-Dox Characterization. *4.3.1. In Vitro Binding Assay.* Approximately 0.6 mg of doxorubicin and an equivalent of IPBA-Dox 1.0 mg were dissolved in 100 μL of DMF and then added to 900 μL of HSA solution (5% in 1× PBS buffer, pH = 7.4). The final mixtures were incubated at 37 °C for 60 min. 200 μL of sample was analyzed by gel filtration chromatography (GFC) on a PD-10 column (G-25) and 1× PBS acting as an eluent buffer. The doxorubicin contents within each collected fractions (ca. 1 mL) were measured by UV−vis spectroscopy at 480 nm. The protein concentrations of the first 7 fractions were determined by a BCA protein assay (Thermo Scientific).

4.3.2. Pharmacokinetic Assay. Animal studies were performed in accordance with protocols approved by the Institutional Animal Care and Use Committee, following their policies and procedures at The Ohio State University (Columbus, OH). 48 ICR healthy male mice were purchased

https://doi.org/10.1021/acsomega.3c07163
ACS Omega 2024, 9, 977−987

from Charles River Laboratory and kept on a 12 h light/dark cycle. Doxorubicin hydrochloride or IPBA-Dox (doxorubicin-equivalent dose) was administered via tail vein IV injection at a single dose of 6.0 mg/kg (MTD of doxorubicin in male ICR mice is approximately 10 mg/kg).[45] Mice were sacrificed at 5, 15, and 30 min, and 1, 2, 4, 24, and 48 h (n = 3 mice per time point), and a minimum of 100 μL of blood was collected from each mouse by cardiac puncture into heparinized vials and stored at −20 °C until analysis. Heart, liver, kidney, stomach, and small intestine tissues were also collected with the remaining blood in those tissues being flushed out by distilled water to minimize the contribution of plasma drug to the result and stored at −80 °C until assayed.

Whole blood (50 μL) was transferred to a 1.5 mL microcentrifuge tube, and 0.6 mL of methanol was added to extract the drugs. The mixtures were vortexed for 15 s, and 0.25 mL of 12 mM phosphoric acid was added. The acidified mixtures were centrifuged at 10,000g for 8 min.[50] The resulting supernatant was collected and adjusted to 1.0 mL for LC−MS/MS analysis (method development in Supporting Information).

The tissues were homogenized in 1 mL of citric acid buffer (pH 6) for 3 min at 3000 rpm. The homogenate was then transferred to a tube containing 3 mL of a solvent mixture (chloroform/methanol = 1:4 v/v). The mixtures were vortexed for 1 min. The organic layers were separated by centrifugation at 2500 rpm for 3 min. Approximately 3 mL of the chloroform layer was transferred to a new tube, and the organic solvent was evaporated to dryness under vacuum. The residues were reconstituted in 200 μL of methanol, and the drug content was analyzed by LC−MS/MS.

The pharmacokinetic parameters of free doxorubicin and IPBA-Dox were calculated using WinNonlin software and a two-compartment model.

4.4. Cell Culture. Human MIAPaCa-2 (MP2) and PANC1 pancreatic carcinoma cells were purchased from the ATCC. Stable pools of shCtrl or shCav1 cells were generated by transfection with nontargeted shRNA (shCtrl) or shRNA targeting Cav-1 (shCav1) and selection with puromycin (1 mg/mL). Mouse KPC and KPC-Cav1$^{-/-}$ pancreatic adenocarcinoma cells were isolated from pancreatic tumors arising in KRAS^{G12D} Trp53^{R270H} PDX1-Cre (KPC) and KRAS^{G12D} Trp53^{R270H} PDX1-Cre−Cav1−/− (KPC-Cav1$^{-/-}$) genetically engineered mice bearing wild-type *CAV1* or homozygous conditional knockout of *CAV1* (complete knockout of Cav-1 protein expression), respectively. All cells were maintained at 37 °C in 5% CO_2 in DMEM supplemented with 10% FBS and 1% penicillin/streptomycin. Cells were not cultured for more than 2 months and were routinely tested for Mycoplasma contamination.

4.5. Cytotoxicity and Colony Forming Assay. Cytotoxicity was measured using alamarBlue reagent following the manufacturer's protocols (BioRad, Oxford, UK), and cells were seeded in 4 replicates in 96-well plates at a density of 1000−3000 cells per well in 100 μL of medium and treated as described. After 72 h, alamarBlue reagent was added and incubated under normal cell culture conditions for 4−8 h, and the fluorescence was read at excitation: 560/20, emission: 590/20.

For colony formation assays, cells were prepared as single-cell suspensions and seeded into 60 mm dishes. After 24 h, the cells were treated with the indicated doses of IPBA-Dox or control for 48 h, after which they were returned to normal growth conditions without chemotherapy and allowed to grow for 10 days. Colonies were then fixed using a methanol/acetic acid solution and stained using a crystal violet solution (0.5%).

4.6. Fluorescence Microscopy. Cells were seeded on 4-well chamber Labtek glass slides (Thermo Scientific, Waltham, MA) in normal growth conditions. Approximately 16 h before treatment, the cells were washed with PBS and changed to serum-free media (0% FBS). One hour before treatment, IPBA-Dox was incubated with HSA at 37 °C (for final 0.5% HSA concentration in well). At the treatment time, IPBA-Dox was diluted in serum-free growth media and added to the cells at a final concentration of 2.5 μM. After 1- or 3 h, cells were washed with two acid/salt solution with 0.1 M glycine and 0.1 M NaCl (pH 3.02) on ice for 2 min each, followed by two washes with PBS. Cells were then fixed with 4% paraformaldehyde and mounted with ProLong Diamond Antifade Mountant with DAPI (Thermo Scientific, Waltham, MA). Images were taken using a Zeiss LSM880 confocal microscope (Zeiss, Oberkochen Germany). Fluorescence signals were quantified by using QuPath software.

4.7. Western Blotting. Whole cell lysates were obtained using RIPA buffer supplemented with octyl-*b*-D-glucopyranoside (Millipore-Sigma St. Louis, MO) and Halt Protease and Phosphatase inhibitor cocktail (Thermo Scientific, Waltham, MA). Proteins were quantified using a DC assay (BioRad, Oxford, UK). Proteins were transferred to PVDF membranes and blocked using 5% milk (Research Products International, Mount Prospect, IL). Cav-1, cleaved caspase 3, actin, and secondary antibodies were purchased from Cell Signaling Technology (Danvers, MA, USA).

4.8. Live-Cell Apoptosis Assay. Cells (1500−2000) in single-cell suspensions were seeded in 96-well plates in triplicate, 24 h before treatment addition. IPBA-Dox was added at final concentrations of 2.5 or 0.1 μM, respectively, for MP2 and PANC1 cells. Media was supplemented with Incucyte Annexin V Green Dye (Sartorius, Goettingen, Germany) and four or more images from each well were taken at least every 4 h using an IncuCyte S3 Live-Cell Analysis System (Sartorius, Goettingen, Germany).

4.9. In Vivo Tumor Growth Study. Following IACUC-approved animal protocols, 2.0 × 10^6 KPC or KPC-Cav-1$^{-/-}$ cells were injected into both subcutaneous flanks in 8−10-week old athymic nude mice balanced for gender (Charles River). The mice were randomly assigned to 3 treatment groups (vehicle, doxorubicin, and IPBA-Dox). Treatment was initiated when tumors reached 100−200 mm^3 in size, and drugs were administered via IV injections once weekly for 3 weeks. A doxorubicin dose of 20 mg/kg or an equivalent dose of IPBA-Dox (IPBA-Dox equivalent to 20 mg/kg of doxorubicin) was dissolved in 0.2 mL of 90% water, 5% DMSO, and 5% Tween 80. Doxorubicin treatment was performed only in mice injected with KPC cells. Each tumor was measured every 2−3 days and volumes were calculated using the formula $L \times W \times W/2$ (L = length, W = width).

4.10. Statistical Analysis. All statistical analyses were performed using GraphPad Prism software. For comparisons, normality was assessed before selecting statistical tests; if it passed, parametric tests were used, or nonparametric tests were used if they failed. The statistical significance threshold was set at p = 0.05. For single variables among two groups, t-test or Mann−Whitney was used, for multiple groups, one-way ANOVA or Kruskal−Wallis with multiple comparisons was used. Two-way analysis of variance was used for two variables.

https://doi.org/10.1021/acsomega.3c07163
ACS Omega 2024, 9, 977−987

For survival analysis, the log-rank Mantel−Cox test was used. Significance is represented as not significant: ns; *: $p < 0.05$; **: $p < 0.01$; ***: $p < 0.001$; ****: $p < 0.0001$.

■ ASSOCIATED CONTENT

Supporting Information

The Supporting Information is available free of charge at https://pubs.acs.org/doi/10.1021/acsomega.3c07163.

Mass spectrometry conditions for doxorubicin, IPBA-Dox, and daunorubicin with representative MS/MS spectra; MS spectra extracted from doxorubicin (544.20, $[M + H]^+$), IPBA-Dox (971.90, $[M + H]^+$), and daunorubicin (528.40, $[M + H]^+$) peaks; pharmacokinetic method validation: (A) chromatogram of a blank plasma sample, (B) calibration curves for quantitation of doxorubicin and IPBA-Dox concentrations in plasma sample, and (C,D) intraday and interday precision and accuracy, recovery, and matrix effect of quality control standards for doxorubicin and IPBA-Dox; and IPBA-Dox is well-tolerated in vivo: (A,B) individual mouse weights were assessed for the duration of the experiment and normalized to that of day 0 (PDF)

■ AUTHOR INFORMATION

Corresponding Authors

Robert J. Lee − *Division of Pharmaceutics and Pharmacology, The Ohio State University, Columbus, Ohio 43210-1132, United States;* orcid.org/0000-0002-5981-5867; Email: lee.1339@osu.edu

Terence M. Williams − *Department of Radiation Oncology, City of Hope National Medical Center, Duarte, California 91010, United States;* orcid.org/0000-0002-1020-0845; Phone: (626) 218-2332; Email: terwilliams@coh.org; Fax: (626) 218-5334

Authors

Yang Liu − *Division of Pharmaceutics and Pharmacology, The Ohio State University, Columbus, Ohio 43210-1132, United States;* orcid.org/0000-0001-8955-4955

Sergio Corrales-Guerrero − *Biomedical Sciences Graduate Program, The Ohio State University, Columbus, Ohio 43210-1132, United States*

Jimmy C. Kuo − *Division of Pharmaceutics and Pharmacology, The Ohio State University, Columbus, Ohio 43210-1132, United States*

Ryan Robb − *University of North Carolina, Chapel Hill, North Carolina 27514-3916, United States*

Gregory Nagy − *Biomedical Sciences Graduate Program, The Ohio State University, Columbus, Ohio 43210-1132, United States*

Tiantian Cui − *Department of Radiation Oncology, City of Hope National Medical Center, Duarte, California 91010, United States*

Complete contact information is available at: https://pubs.acs.org/10.1021/acsomega.3c07163

Author Contributions

⊥Y. Liu: conceptualization, methodology, investigation, validation, formal analysis, writing-original draft, writing-review, and editing. S. Corrales-Guerrero: conceptualization, methodology, investigation, validation, formal analysis, writing-original draft, writing-review, and editing. J. C. Kuo: methodology, investigation, writing-review, and editing. R. Robb: methodology, investigation, writing-review, and editing. G. Nagy: methodology, investigation, writing-review, and editing. T. Cui: writing review and editing. R. J. Lee: conceptualization, resources, formal analysis, supervision, funding acquisition, validation, investigation, methodology, writing-original draft, writing-review, and editing. T. M. Williams: conceptualization, resources, formal analysis, supervision, funding acquisition, validation, investigation, methodology, writing-original draft, writing-review, and editing. Yang Liu and Sergio Corrales-Guerrero contributed equally.

Notes

The authors declare no competing financial interest.

■ ACKNOWLEDGMENTS

This work was supported by the following grants: NIH R01 CA198128-01 (T.W. and R.L.). Research reported in this article was also supported by The Ohio State University Comprehensive Cancer Center (OSU-CCC) (P30 CA016058) and the City of Hope Comprehensive Cancer Center (COH-CCC) (P30 CA033572).

■ REFERENCES

(1) Sleep, D.; Cameron, J.; Evans, L. R. Albumin as a versatile platform for drug half-life extension. *Biochim. Biophys. Acta* **2013**, *1830*, 5526−5534.

(2) Garmann, D.; Warnecke, A.; Kalayda, G. V.; Kratz, F.; Jaehde, U. Cellular accumulation and cytotoxicity of macromolecular platinum complexes in cisplatin-resistant tumor cells. *J. Controlled Release* **2008**, *131*, 100−106.

(3) Yang, F.; Liang, H. Editorial (Thematic Issue: HSA-Based Drug Development and Drug Delivery Systems). *Curr. Pharm. Des.* **2015**, *21*, 1784.

(4) Kobayashi, H.; Watanabe, R.; Choyke, P. L. Improving conventional enhanced permeability and retention (epr) effects; what is the appropriate target? *Theranostics* **2014**, *4*, 81−89.

(5) Ojha, T.; Pathak, V.; Shi, Y.; Hennink, W. E.; Moonen, C. T.; Storm, G.; Kiessling, F.; Lammers, T. Pharmacological and physical vessel modulation strategies to improve epr-mediated drug targeting to tumors. *Adv. Drug Deliv. Rev.* **2017**, *119*, 44−60.

(6) Golombek, S. K.; May, J. N.; Theek, B.; Appold, L.; Drude, N.; Kiessling, F.; Lammers, T. Tumor targeting via epr: Strategies to enhance patient responses. *Adv. Drug Deliv. Rev.* **2018**, *130*, 17−38.

(7) Chatterjee, M.; Ben-Josef, E.; Robb, R.; Vedaie, M.; Seum, S.; Thirumoorthy, K.; Palanichamy, K.; Harbrecht, M.; Chakravarti, A.; Williams, T. M. Caveolae-mediated endocytosis is critical for albumin cellular uptake and response to albumin-bound chemotherapy. *Cancer Res.* **2017**, *77*, 5925−5937.

(8) Hoogenboezem, E. N.; Duvall, C. L. Harnessing albumin as a carrier for cancer therapies. *Adv. Drug Deliv. Rev.* **2018**, *130*, 73−89.

(9) Mo, Y.; Barnett, M. E.; Takemoto, D.; et al. Human serum albumin nanoparticles for efficient delivery of cu, zn superoxide dismutase gene. *Mol. Vis.* **2007**, *13*, 746−757.

(10) Schnitzer, J. E.; Carley, W. W.; Palade, G. E. Albumin interacts specifically with a 60-kda microvascular endothelial glycoprotein. *Proc. Natl. Acad. Sci. U.S.A.* **1988**, *85*, 6773−6777.

(11) Schnitzer, J. E.; Oh, P. Antibodies to sparc inhibit albumin binding to sparc, gp60, and microvascular endothelium. *Am. J. Physiol.* **1992**, *263*, H1872−H1879.

(12) Robb, R.; Kuo, J. C.; Liu, Y.; Corrales-Guerrero, S.; Cui, T.; Hegazi, A.; Nagy, G.; Lee, R. J.; Williams, T. M. A novel protein-drug conjugate, ssh20, demonstrates significant efficacy in caveolin-1-expressing tumors. *Mol. Ther.-Oncolytics* **2021**, *22*, 555−564.

(13) Razani, B.; Woodman, S. E.; Lisanti, M. P. Caveolae: From cell biology to animal physiology. *Pharmacol. Rev.* **2002**, *54*, 431−467.

(14) Williams, T. M.; Lisanti, M. P. The caveolin genes: From cell biology to medicine. *Ann. Med.* **2004**, *36*, 584−595.
(15) Williams, T. M.; Lisanti, M. P. Caveolin-1 in oncogenic transformation, cancer, and metastasis. *Am. J. Physiol. Cell Physiol.* **2005**, *288*, C494−C506.
(16) Yang, G.; Truong, L. D.; Timme, T. L.; et al. Elevated expression of caveolin is associated with prostate and breast cancer. *Clin. Cancer Res.* **1998**, *4*, 1873−1880.
(17) Kato, K.; Hida, Y.; Miyamoto, M.; Hashida, H.; Shinohara, T.; Itoh, T.; Okushiba, S.; Kondo, S.; Katoh, H. Overexpression of caveolin-1 in esophageal squamous cell carcinoma correlates with lymph node metastasis and pathologic stage. *Cancer* **2002**, *94*, 929−933.
(18) Yoo, S. H.; Park, Y. S.; Kim, H. R.; Sung, S. W.; Kim, J. H.; Shim, Y. S.; Lee, S. D.; Choi, Y. L.; Kim, M. K.; Chung, D. H. Expression of caveolin-1 is associated with poor prognosis of patients with squamous cell carcinoma of the lung. *Lung Cancer* **2003**, *42*, 195−202.
(19) Zhan, P.; Shen, X. K.; Qian, Q.; Wang, Q.; Zhu, J. P.; Zhang, Y.; Xie, H. Y.; Xu, C. H.; Hao, K. K.; Hu, W.; et al. Expression of caveolin-1 is correlated with disease stage and survival in lung adenocarcinomas. *Oncol. Rep.* **2012**, *27*, 1072−1078.
(20) Chatterjee, M.; Ben-Josef, E.; Thomas, D. G.; Morgan, M. A.; Zalupski, M. M.; Khan, G.; Andrew Robinson, C.; Griffith, K. A.; Chen, C. S.; Ludwig, T.; et al. Caveolin-1 is associated with tumor progression and confers a multi-modality resistance phenotype in pancreatic cancer. *Sci. Rep.* **2015**, *5*, 10867.
(21) Suzuoki, M.; Miyamoto, M.; Kato, K.; Hiraoka, K.; Oshikiri, T.; Nakakubo, Y.; Fukunaga, A.; Shichinohe, T.; Shinohara, T.; Itoh, T.; et al. Impact of caveolin-1 expression on prognosis of pancreatic ductal adenocarcinoma. *Br. J. Cancer* **2002**, *87*, 1140−1144.
(22) Cordes, N.; Frick, S.; Brunner, T. B.; Pilarsky, C.; Grützmann, R.; Sipos, B.; Klöppel, G.; McKenna, W. G.; Bernhard, E. J. Human pancreatic tumor cells are sensitized to ionizing radiation by knockdown of caveolin-1. *Oncogene* **2007**, *26*, 6851−6862.
(23) Li, L.; Yang, G.; Ebara, S.; et al. Caveolin-1 mediates testosterone-stimulated survival/clonal growth and promotes metastatic activities in prostate cancer cells. *Cancer Res.* **2001**, *61*, 4386−4392.
(24) Ho, C. C.; Huang, P. H.; Huang, H. Y.; Chen, Y. H.; Yang, P. C.; Hsu, S. M. Up-regulated caveolin-1 accentuates the metastasis capability of lung adenocarcinoma by inducing filopodia formation. *Am. J. Pathol.* **2002**, *161*, 1647−1656.
(25) Williams, T. M.; Hassan, G. S.; Li, J.; Cohen, A. W.; Medina, F.; Frank, P. G.; Pestell, R. G.; Di Vizio, D.; Loda, M.; Lisanti, M. P. Caveolin-1 promotes tumor progression in an autochthonous mouse model of prostate cancer: Genetic ablation of cav-1 delays advanced prostate tumor development in tramp mice. *J. Biol. Chem.* **2005**, *280*, 25134−25145.
(26) Ho, C. C.; Kuo, S. H.; Huang, P. H.; Huang, H. Y.; Yang, C. H.; Yang, P. C. Caveolin-1 expression is significantly associated with drug resistance and poor prognosis in advanced non-small cell lung cancer patients treated with gemcitabine-based chemotherapy. *Lung Cancer* **2008**, *59*, 105−110.
(27) Li, M.; Chen, H.; Diao, L.; Zhang, Y.; Xia, C.; Yang, F. Caveolin-1 and vegf-c promote lymph node metastasis in the absence of intratumoral lymphangiogenesis in non-small cell lung cancer. *Tumori* **2010**, *96*, 734−743.
(28) Cui, T.; Corrales-Guerrero, S.; Castro-Aceituno, V.; Nair, S.; Maneval, D. C.; Monnig, C.; Kearney, P.; Ellis, S.; Raheja, N.; Raheja, N.; et al. Jntx-101, a novel albumin-encapsulated gemcitabine prodrug, is efficacious and operates via caveolin-1-mediated endocytosis. *Mol. Ther.-Oncolytics* **2023**, *30*, 181−192.
(29) Bertino, E. M.; Williams, T. M.; Nana-Sinkam, S. P.; Shilo, K.; Chatterjee, M.; Mo, X.; Rahmani, M.; Phillips, G. S.; Villalona-Calero, M. A.; Otterson, G. A. Stromal caveolin-1 is associated with response and survival in a phase ii trial of nab-paclitaxel with carboplatin for advanced nsclc patients. *Clin. Lung Cancer* **2015**, *16*, 466−474.e4.
(30) Williams, T. M.; Schneeweiss, A.; Jackisch, C.; Shen, C.; Weber, K. E.; Fasching, P. A.; Denkert, C.; Furlanetto, J.; Heinmöller, E.; Schmatloch, S.; et al. Caveolin gene expression predicts clinical outcomes for early-stage her2-negative breast cancer treated with paclitaxel-based chemotherapy in the geparsepto trial. *Clin. Cancer Res.* **2023**, *29*, 3384−3394.
(31) Zhao, Y. N.; Lv, F. F.; Chen, S.; et al. Caveolin-1 expression predicts efficacy of weekly nab-paclitaxel plus gemcitabine for metastatic breast cancer in the phase ii clinical trial. *BMC Cancer* **2018**, *18*, 1019.
(32) Hortobágyi, G. N. Anthracyclines in the treatment of cancer. An overview. *Drugs* **1997**, *54* (Suppl 4), 1−7.
(33) Chatterjee, K.; Zhang, J.; Honbo, N.; Karliner, J. S. Doxorubicin cardiomyopathy. *Cardiology* **2010**, *115*, 155−162.
(34) Cagel, M.; Grotz, E.; Bernabeu, E.; Moretton, M. A.; Chiappetta, D. A. Doxorubicin: Nanotechnological overviews from bench to bedside. *Drug Discov. Today* **2017**, *22*, 270−281.
(35) Yesair, D. W.; Schwartzbach, E.; Shuck, D.; et al. Comparative pharmacokinetics of daunomycin and adriamycin in several animal species. *Cancer Res.* **1972**, *32*, 1177−1183.
(36) Green, A. E.; Rose, P. G. Pegylated liposomal doxorubicin in ovarian cancer. *Int. J. Nanomed.* **2006**, *1*, 229−239.
(37) Susa, M.; Iyer, A. K.; Ryu, K.; Hornicek, F. J.; Mankin, H.; Amiji, M. M.; Duan, Z. Doxorubicin loaded polymeric nanoparticulate delivery system to overcome drug resistance in osteosarcoma. *BMC Cancer* **2009**, *9*, 399.
(38) Shaikh, M. V.; Kala, M.; Nivsarkar, M. Formulation and optimization of doxorubicin loaded polymeric nanoparticles using box-behnken design: Ex-vivo stability and in-vitro activity. *Eur. J. Pharm. Sci.* **2017**, *100*, 262−272.
(39) Sapra, P.; Stein, R.; Pickett, J.; Qu, Z.; Govindan, S. V.; Cardillo, T. M.; Hansen, H. J.; Horak, I. D.; Griffiths, G. L.; Goldenberg, D. M. Anti-cd74 antibody-doxorubicin conjugate, immu-110, in a human multiple myeloma xenograft and in monkeys. *Clin. Cancer Res.* **2005**, *11*, 5257−5264.
(40) Yeh, M. Y.; Roffler, S. R.; Yu, M. H. Doxorubicin: Monoclonal antibody conjugate for therapy of human cervical carcinoma. *Int. J. Cancer* **1992**, *51*, 274−282.
(41) DeFeo-Jones, D.; Garsky, V. M.; Wong, B. K.; Feng, D. M.; Bolyar, T.; Haskell, K.; Kiefer, D. M.; Leander, K.; McAvoy, E.; Lumma, P.; et al. A peptide-doxorubicin 'prodrug' activated by prostate-specific antigen selectively kills prostate tumor cells positive for prostate-specific antigen in vivo. *Nat. Med.* **2000**, *6*, 1248−1252.
(42) Du, C.; Deng, D.; Shan, L.; Wan, S.; Cao, J.; Tian, J.; Achilefu, S.; Gu, Y. A ph-sensitive doxorubicin prodrug based on folate-conjugated bsa for tumor-targeted drug delivery. *Biomaterials* **2013**, *34*, 3087−3097.
(43) Chen, X.; Parelkar, S. S.; Henchey, E.; Schneider, S.; Emrick, T. Polympc-doxorubicin prodrugs. *Bioconjugate Chem.* **2012**, *23*, 1753−1763.
(44) Kratz, F.; Mansour, A.; Soltau, J.; Warnecke, A.; Fichtner, I.; Unger, C.; Drevs, J. Development of albumin-binding doxorubicin prodrugs that are cleaved by prostate-specific antigen. *Arch. Pharm.* **2005**, *338*, 462−472.
(45) Yuan, A.; Wu, J.; Song, C.; Tang, X.; Qiao, Q.; Zhao, L.; Gong, G.; Hu, Y. A novel self-assembly albumin nanocarrier for reducing doxorubicin-mediated cardiotoxicity. *J. Pharm. Sci.* **2013**, *102*, 1626−1635.
(46) Ibsen, S.; Su, Y.; Norton, J.; Zahavy, E.; Hayashi, T.; Adams, S.; Wrasidlo, W.; Esener, S. Extraction protocol and mass spectrometry method for quantification of doxorubicin released locally from prodrugs in tumor tissue. *J. Mass Spectrom.* **2013**, *48*, 768−773.
(47) Rahman, A.; Carmichael, D.; Harris, M.; et al. Comparative pharmacokinetics of free doxorubicin and doxorubicin entrapped in cardiolipin liposomes. *Cancer Res.* **1986**, *46*, 2295−2299.
(48) Tiruppathi, C.; Song, W.; Bergenfeldt, M.; Sass, P.; Malik, A. B. Gp60 activation mediates albumin transcytosis in endothelial cells by tyrosine kinase-dependent pathway. *J. Biol. Chem.* **1997**, *272*, 25968−25975.

https://doi.org/10.1021/acsomega.3c07163
ACS Omega 2024, 9, 977−987

(49) Tiruppathi, C.; Finnegan, A.; Malik, A. B. Isolation and characterization of a cell surface albumin-binding protein from vascular endothelial cells. *Proc. Natl. Acad. Sci. U.S.A.* **1996**, *93*, 250−254.
(50) Gustafson, D. L.; Rastatter, J. C.; Colombo, T.; Long, M. E. Doxorubicin pharmacokinetics: Macromolecule binding, metabolism, and excretion in the context of a physiologic model. *J. Pharm. Sci.* **2002**, *91*, 1488−1501.
(51) Formelli, F.; Pollini, C.; Casazza, A. M.; di Marco, A.; Mariani, A. Fluorescence assays and pharmacokinetic studies of 4'-deoxydoxorubicin and doxorubicin in organs of mice bearing solid tumors. *Cancer Chemother. Pharmacol.* **1981**, *5*, 139−144.
(52) Lee, R. J.; Lee, R. J.; Yung, B.; Li, H.; Zhou, C.; Lee, L. Lactosylated liposomes for targeted delivery of doxorubicin to hepatocellular carcinoma. *Int. J. Nanomed.* **2012**, *7*, 5465−5474.
(53) Daeihamed, M.; Haeri, A.; Dadashzadeh, S. A simple and sensitive hplc method for fluorescence quantitation of doxorubicin in micro-volume plasma: Applications to pharmacokinetic studies in rats. *Iran. J. Pharm. Res.* **2015**, *14*, 33−42.
(54) Kratz, F.; Warnecke, A.; Scheuermann, K.; Stockmar, C.; Schwab, J.; Lazar, P.; Drückes, P.; Esser, N.; Drevs, J.; Rognan, D.; et al. Probing the cysteine-34 position of endogenous serum albumin with thiol-binding doxorubicin derivatives. Improved efficacy of an acid-sensitive doxorubicin derivative with specific albumin-binding properties compared to that of the parent compound. *J. Med. Chem.* **2002**, *45*, 5523−5533.
(55) Kratz, F.; Müller-Driver, R.; Hofmann, I.; Drevs, J.; Unger, C. A novel macromolecular prodrug concept exploiting endogenous serum albumin as a drug carrier for cancer chemotherapy. *J. Med. Chem.* **2000**, *43*, 1253−1256.
(56) Trüssel, S.; Dumelin, C.; Frey, K.; Villa, A.; Buller, F.; Neri, D. New strategy for the extension of the serum half-life of antibody fragments. *Bioconjugate Chem.* **2009**, *20*, 2286−2292.
(57) Werle, M.; Bernkop-Schnürch, A. Strategies to improve plasma half life time of peptide and protein drugs. *Amino Acids* **2006**, *30*, 351−367.
(58) Dumelin, C. E.; Trüssel, S.; Buller, F.; Trachsel, E.; Bootz, F.; Zhang, Y.; Mannocci, L.; Beck, S.; Drumea-Mirancea, M.; Seeliger, M.; et al. A portable albumin binder from a DNA-encoded chemical library. *Angew. Chem., Int. Ed. Engl.* **2008**, *47*, 3196−3201.

https://doi.org/10.1021/acsomega.3c07163
ACS Omega 2024, 9, 977−987